FEBS Open Bio 5 (2015) 885–892

journal homepage: www.elsevier.com/locate/febsopenbio

Kinetic studies on the oxidation of semiquinone and hydroquinone forms of *Arabidopsis* cryptochrome by molecular oxygen

Luuk J.G.W. van Wilderen [a,*], Gary Silkstone [b], Maria Mason [b], Jasper J. van Thor [a], Michael T. Wilson [b]

[a] Division of Molecular Biosciences, Faculty of Natural Sciences, South Kensington Campus, Imperial College London, London, United Kingdom
[b] Department of Biological Sciences, University of Essex, Wivenhoe Park, Colchester, United Kingdom

ARTICLE INFO

Article history:
Received 15 September 2015
Revised 18 October 2015
Accepted 20 October 2015

Keywords:
Stopped-flow
Flavin adenine dinucleotide
Photoreduction
Spectroscopy
Global analysis
Flavin hydroperoxide

ABSTRACT

Cryptochromes (crys) are flavoprotein photoreceptors present throughout the biological kingdom that play important roles in plant development and entrainment of the circadian clock in several organisms. Crys non-covalently bind flavin adenine dinucleotide (FAD) which undergoes photoreduction from the oxidised state to a radical form suggested to be active in signalling *in vivo*. Although the photoreduction reactions have been well characterised by a number of approaches, little is known of the oxidation reactions of crys and their mechanisms. In this work, a stopped-flow kinetics approach is used to investigate the mechanism of cry oxidation in the presence and absence of an external electron donor. This *in vitro* study extends earlier investigations of the oxidation of *Arabidopsis* cryptochrome1 by molecular oxygen and demonstrates that, under some conditions, a more complex model for oxidation of the flavin than was previously proposed is required to accommodate the spectral evidence (see P. Müller and M. Ahmad (2011) J. Biol. Chem. 286, 21033–21040 [1]). In the absence of an electron donor, photoreduction leads predominantly to the formation of the radical FADH$^{\cdot}$. Dark recovery most likely forms flavin hydroperoxide (FADHOOH) requiring superoxide. In the presence of reductant (DTT), illumination yields the fully reduced flavin species (FADH^{-}). Reaction of this with dioxygen leads to transient radical (FADH$^{\cdot}$) and simultaneous accumulation of oxidised species (FAD), possibly governed by interplay between different cryptochrome molecules or cooperativity effects within the cry homodimer.

1. Introduction

Cryptochromes are flavin-binding proteins that are blue light photoreceptors, implicated in the circadian clock and multiple developmental roles in humans, plants, bacteria and animals [2–5]. In addition to the primary FAD chromophore, there is evidence that cry possesses a pterin molecule (methenyltetrahydrofolate; MTHF), suggested to act as a light harvesting antenna [6]. Although cry has a high degree of homology with photolyases [2], it does not share the DNA-lesion repair capabilities of its family member (except for cry-DASH that repairs single-stranded DNA [7]). Unlike photolyases, where flavins are generally reduced [8], cryptochromes appear to contain flavin in the fully oxidised state in the dark (resting state). The fully reduced state is inactive and not favoured *in vivo* [9,10] and in fact requires the presence of reducing agent for its formation *in vitro* [11]. Upon illumination, electron transfer from a nearby Trp residue to an excited state of flavin occurs, generating the neutral radical form in plants (*Arabidopsis* cry1 and cry2) and the anionic radical in animals (drosophila and human crys), thus forming the activated signalling state [12–15]. Upon transfer to darkness, cry reoxidation seems to occur spontaneously to regenerate the oxidised flavin (resting state). The degree of activation of crys therefore depends on the equilibrium reached under illumination conditions between the forward (photoreduction) reaction and the reverse (oxidation) reaction of flavin, and both forward and reverse reactions are essential for photoreceptor function. Although numerous studies exist on the mechanisms involved in the forward (light activation) reactions of cryptochromes and the related photolyases [2,14,16], the mechanism of the flavin oxidation (dark inactivation) reaction either *in vivo* or *in vitro* is virtually unexamined. To the best of our

Abbreviations: crys, cryptochromes; DTT, dithiothreitol; FAD, flavin adenine dinucleotide; FADHOOH, flavin hydroperoxide; MTHF, methenyltetrahydrofolate; NOS, nitric oxide synthase

* Corresponding author at: Wolfgang Goethe University Frankfurt, Max-von-Laue-Strasse 1, 60438 Frankfurt am Main, Germany. Tel.: +49 69 798 46409; fax: +49 69 798 46421.

E-mail address: vanwilderen@biophysik.org (L.J.G.W. van Wilderen).

http://dx.doi.org/10.1016/j.fob.2015.10.007
2211-5463/

knowledge, only one similar study has been reported (with reductant only) [1]. Here we present studies that extend earlier work by collecting kinetic data with ms time resolution as opposed to the minute regime reported earlier. These investigations show that, under our conditions with or without reductant the earlier proposed mechanism for oxidation of the fully reduced flavin cannot adequately account for the kinetic profiles observed.

Current views of the mechanism of oxidation propose that reduced flavin donates an electron to O_2 to form the flavin radical and the superoxide anion, $O_2^{\cdot-}$. This step is generally rate limiting and in the order of 250 M^{-1} s^{-1} for free flavins [17]. Radical formation is followed by the formation of H_2O_2 and the oxidised flavin, (directly, or via a C(4a) hydroperoxide intermediate in some proteins) [17,18]. In order to form the oxidised flavin, molecular oxygen needs to gain access to the chromophore from the solvent. In general oxygen may diffuse through proteins via tunnels and cavities that arise due to thermal motion of the protein [19]. The transitions between the different redox states can conveniently be followed by spectroscopic methods, as FAD in the oxidised state has typical absorption maxima at 375 and 450 nm (11,000 M^{-1} cm^{-1}), [20,21] and the reduced form has λ_{max} = 250 nm with shoulders around 280 and 400 nm [22]. The radical form, the semiquinone, might occur either in a neutral form, absorbing between 580 and 620 nm (4,000 M^{-1} cm^{-1}) or an anionic form, absorbing at 380 nm (16,000 M^{-1} cm^{-1}) with a sharp peak at 400 nm and a smaller but broader peak at 490 nm [23,24]. The MTHF antenna absorbs around 380–410 nm (20–25,000 M^{-1} cm^{-1}) [25,26], but is absent from our samples.

In this study we present a detailed stopped-flow spectroscopic investigation of the optical transitions and associated kinetics of the reaction between molecular oxygen and photoreduced cryptochrome. In addition, oxygen electrode studies show that, upon blue light illumination, oxygen is consumed to produce H_2O_2, confirming earlier work [1]. The results presented are relevant for cryptochrome's function in general, and have important implications for the possible role of cry to act as a sensor of the geomagnetic field using a radical pair mechanism [27–29]. This process requires the presence of a flavin radical and a radical partner, which may be superoxide [30], a common transient product in the molecular activation of flavins and flavoproteins [17,31]. The present study extends earlier investigations and provides important new information to assist in the identification of mechanistic pathways that may govern radical pair formation and decay. For instance, a simultaneous production of the radical and oxidised forms is observed from the fully reduced flavin species in presence of reductant, and the neutral radical is found to predominantly form the oxidised state in absence of an external electron donor. A second product of the latter reaction is most likely FADHOOH, requiring superoxide, potentially representing the flavin's radical partner. For the first time, this study presents the reaction mechanisms for oxidation of both partially (flavin radical) and fully reduced cry by molecular oxygen.

2. Results

2.1. The reaction of molecular oxygen with photoreduced cry in the absence of reducing agents

Arabidopsis cry1 was photoreduced under anaerobic conditions in either Tris buffer, or Phosphate buffer in the absence of added reductant. Under these conditions and independently of buffer type, cry is reduced on illumination to form the flavin neutral radical state and does not undergo additional photoconversion to the fully reduced form. On mixing the radical form with oxygen in a stopped-flow spectrometer spectral transitions were observed as depicted in Fig. 1.

A clear isosbestic point around 485 nm in Fig. 1A indicates a transition between two dominant states, the radical (absorbing from around 500–650 nm) and the oxidised form (peaks at 380, 445 and 469 nm, and a shoulder around 417 nm). No other intermediates are observed, indicating that the fully reduced species is scarcely formed, or can at most be a minor contributing species. Oxidation of the radical state is relatively slow, occurring over a time scale of several minutes. However, its oxidation does not require additional oxidising agents like iodine as is typical for certain photolyases [32].

Fig. 1B illustrates the time courses of the spectral transitions depicted in Fig. 1A over a range of oxygen concentrations. For clarity a subset of the data collected is shown. This figure demonstrates that the rate constant for the reaction exhibits an oxygen concentration dependence. This is most easily seen when the apparent rate constant for the overall reaction ($k_{obs} = \ln 2/t_h$, t_h being the time to reach 50% of the amplitude reached at 500 s and therefore independent of differences in extinction coefficients) is plotted as a function of the oxygen concentration. This is provided in panel C. It is seen that the rate constant has a linear dependence on the oxygen concentration yielding an apparent second order rate constant of about 64 M^{-1} s^{-1}, independent of wavelength (i.e. at 450 and 532 nm the slope is near identical). Interestingly, the radical disappears more slowly than oxidised FAD is formed (i.e. k_{obs} at 532 nm is smaller than k_{obs} at 450 nm, independent of the oxygen concentration used). The small difference in the oxygen-independent rate constant seen at 450 and 532 nm is likely a consequence of expressing a complex reaction (e.g. more than one species absorbs at 450 nm) in terms of a single half time. In fact, global analysis on this data (see below) shows that more than one species, absorbing at 450 nm, is formed from the radical species. Moreover the intercept on the ordinate at both wavelengths suggests a pre-equilibrium in which oxygen is weakly bound (i.e. caused by an additional process, which may consist of the binding of oxygen prior to the redox reaction, and exhibit an oxygen-independent rate constant which is added to k_{obs} thereby introducing the vertical offset) and the intercept may thus be a parameter incorporating the oxygen dissociation rate constant (see for instance Ref. [33] for an example regarding pre-equilibrium rate kinetics).

2.2. The reaction of molecular oxygen with photoreduced cry in the presence of a reducing agent

In the presence of a reducing agent blue light illumination of cry yielded the fully reduced species irrespective of buffer composition, phosphate or Tris. However, the spectral transitions and associated time courses observed on mixing reduced cry with oxygen did depend on the buffer chosen. Fig. 2 shows the reaction in phosphate buffer and it is seen that there is a transition from the fully reduced species to the oxidised form. In addition, the participation of a radical intermediate through the absorbance changes in the 500–600 nm range can be discerned (depicted by arrow 1). The time courses associated with the spectral transitions seen in this figure are given in Fig. 2B. Whereas the time courses at 450 nm are reminiscent of those shown in Fig. 1, the time courses collected at 532 nm are distinctly different. Here we see a small initial decrease in absorbance assigned to the radical species (not visible in the subset of the shown data in Fig. 2B due to the used time step of 48 s per spectrum) followed by a substantial increase which in turn leads to a bleaching of this absorbance at longer times (Fig. 2B, lower panel). The initial decrease over the first 5 s is similar to that seen in the absence of reductant (Fig. 1B, lower panel) where the time course reports the oxidation of the radical and indicates that some radical was present in the beginning of the experiment.

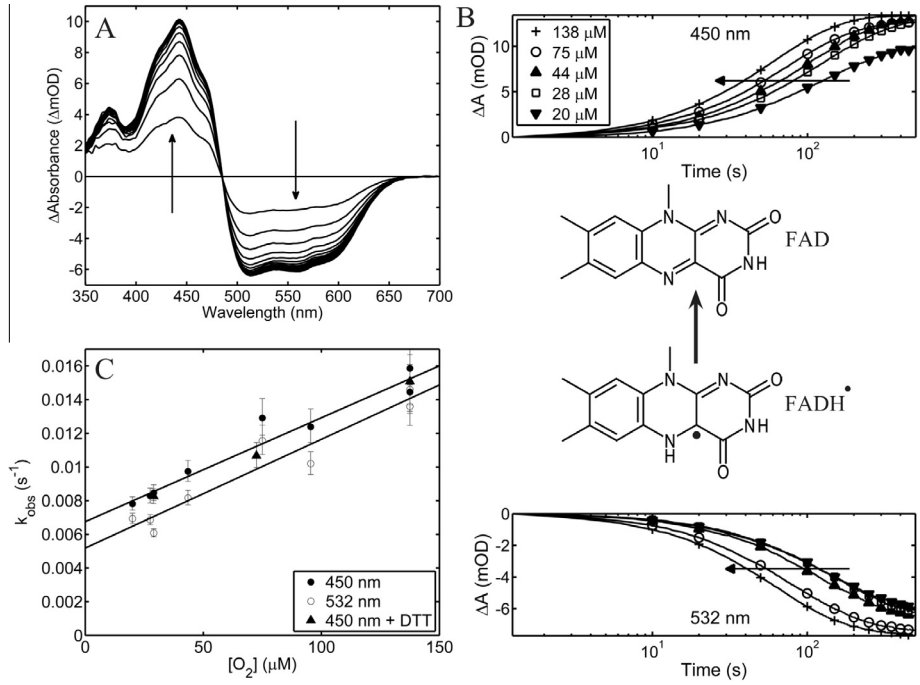

Fig. 1. Oxidation of photoreduced cry without reductant. Panel A. Absorption difference spectra for oxidation of photoreduced cry by oxygen (138 μM) in the absence of reductant. A subset of the available spectra from 1.25 to 476 s is shown in 25 s steps. The arrows indicate the time evolution of the spectra. Panel B. Time courses of the data shown in panel A at 450 nm (upper graph) and 532 nm (lower graph) collected at a number of oxygen concentrations (Tris buffer). The chemical structures corresponding to the flavin redox states that predominantly absorb at these wavelengths are also shown. The arrows denote the trend for increasing oxygen concentration. Panel C shows the apparent observed rate constant (k_{obs}) for oxidation as function of the oxygen concentration. At 450 nm k_{obs} was determined in both buffer types, and at 532 nm for Tris buffer only (see text). The continuous lines represent their respective (buffer independent) weighted linear fits (having slopes of 62 and 65 M^{-1} s^{-1}). Error bars are also given for k_{obs}.

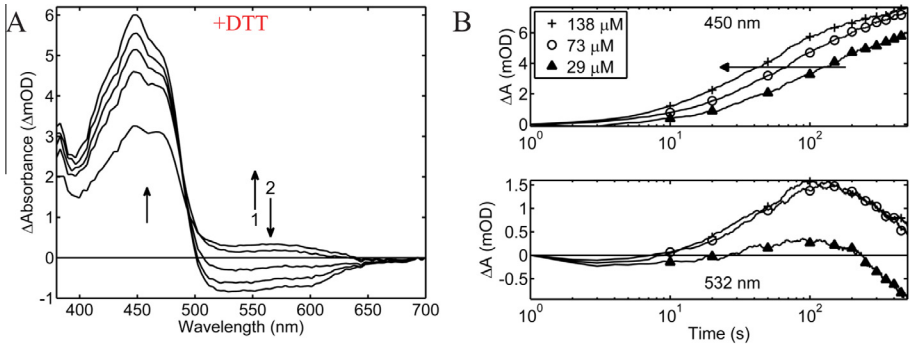

Fig. 2. Oxidation of photoreduced cry in the presence of reductant. Panel A. Absorption difference spectra for oxidation of photoreduced cry in the presence of 3 mM DTT reductant (in phosphate buffer). A subset of the available spectra from 1.25 to 476 s is shown in 48 s steps after mixing with oxygen (29 μM). The arrows indicate the time evolution of the spectra. The numbers indicate the increase from 10 to 100 s (number 1), and the subsequent decrease in the radical signal after 100 s (number 2). Note therefore that the initial decrease at 532 nm from 1 to 10 s is not shown. Panel B. Time courses of the oxidation of data shown in panel A at 450 nm (upper) and 532 nm (lower) collected at a number of oxygen concentrations. The arrow denotes the trend for increasing oxygen concentration.

Once again, the rate of formation of oxidised FAD was dependent on the oxygen concentration and this rate was not significantly different from those obtained with either phosphate or Tris containing buffers on the absence of reductant (see the 450 nm traces in Fig. 1C). Comparable experiments in Tris buffer with reductant exhibited a different oxygen concentration dependence from that seen in phosphate. It is known that Tris is not an innocent buffer for the study of some types of mechanisms that involve radicals [34] and this confounds an analysis of the data. We will therefore focus on the phosphate buffer (but show the results in Tris in Fig. S1 nevertheless).

2.3. Oxygen consumption by cry on blue light illumination and product identification

Having identified O_2 as being essential for the oxidation in cry with reductant an oxygen electrode experiment was performed to inquire if superoxide was formed during this redox reaction. Consistent with earlier work [1] the oxygen concentration fell linearly during the period of illumination and ceased to fall when illumination ended. Addition of superoxide dismutase (catalysing the formation of hydrogen peroxide from superoxide) led to essentially no increase of oxygen concentration in solution. Addition of

catalase however led to a substantial increase in oxygen concentration, indicating that catalase was producing oxygen from hydrogen peroxide formed from the earlier redox reaction between reduced cry molecular oxygen.

2.4. Global analysis reveals that the pathway of oxidation depends on whether reductant is present or absent

Although the central features of the reaction can be appreciated by consideration of single wavelength traces (see above) a more powerful approach of global analysis allows further important mechanistic details to be discerned and possible mechanisms assigned. Such analyses reveal that reactions of reduced and partially reduced cryptochrome with oxygen are indeed complex. In Fig. 3 we have employed global analysis to extract time-independent spectra of intermediates. However, such spectra depend upon choice of model to fit the data (see Materials and Methods). Here we have used two simple models, which allow one to visualise spectral intermediates. In this figure we have analysed the raw data given in Figs. 1 and 2 by both sequential and parallel mechanisms.

The spectra resulting from the application of a sequential model (Fig. 3A; no reductant, 38 μM O_2) shows the disappearance of the radical species (absorbing from 500 to 650 nm), and the simultaneous formation of the oxidised form (445 nm and a shoulder at 475 nm). Also, in the cyan end spectrum (which represents the final measured difference spectrum) the absorption bands corresponding to the oxidised species show an apparent blue shift (to 423 nm and 453 nm, denoted by the arrows) compared to the oxidised species (note also that this shift is even more evident when the parallel model is applied, see Fig. 3B). This is consistent with the formation of flavin hydroperoxide, which typically exhibits a 10–15 nm blue shift [35,36]. This blue shift takes place in the red to the cyan transition (k_{CD} in Fig. 3A). If the parallel model is applied to the same data set (Fig. 3B) it is apparent that the 107 s component (in green) is associated with the radical to oxidised transition (k_{BD}), i.e. a decrease in the 500–650 nm region and an increase in the sub-500 nm region. The differences in spectral distribution in the 500–650 nm region between the 107 s and long-lived components apparently show that the radical species are different, i.e. in this spectral region the green and red spectra exhibit different maxima. However, this may be due to spectral overlap with a blue-absorbing species for the long-lived spectrum. With this analysis in mind we favour the parallel model (Fig. 3B) over the sequential one (Fig. 3A), because the latter results in (very similar) spectra that share features over the whole spectral range, while the parallel model results in three unique basis spectra. Thus the parallel model provides spectral information more compatible with the known distinct spectral properties of the chemical species present (e.g. oxidised, semi-reduced etc).

Global analysis also yields the oxygen concentration dependences of the rate constants for the processes described above. Fig. 4 shows the results of this analysis in which the fitted rate constants for the processes seen in the absence of reducing agent are plotted as a function of oxygen concentration. The two faster processes have rate constants linearly dependent on oxygen

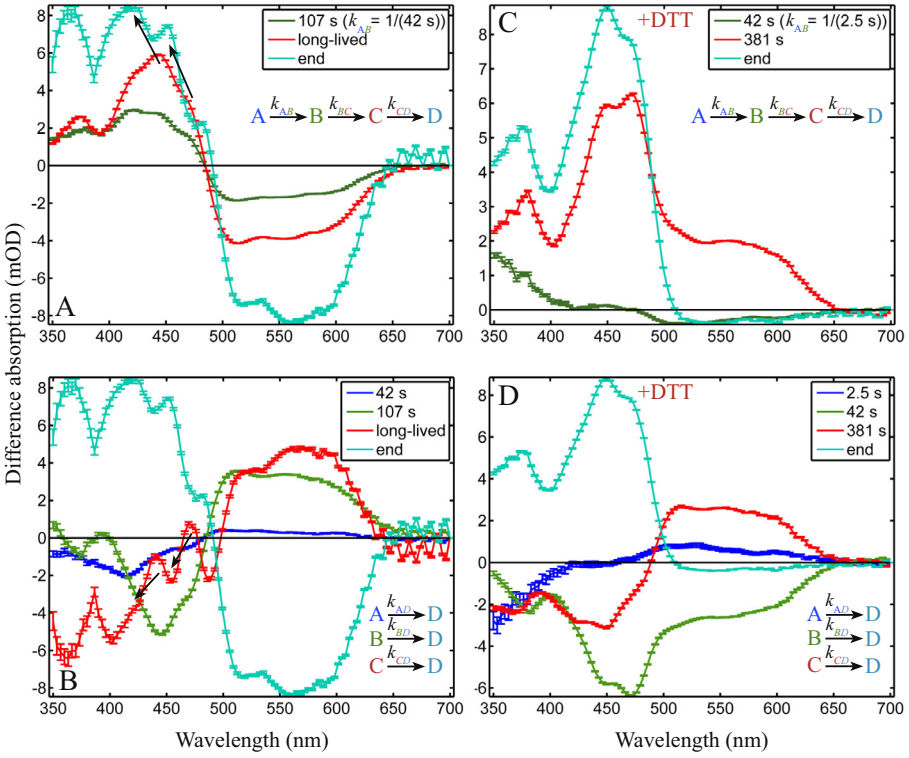

Fig. 3. Spectra resulting from global analysis of time-dependent data after mixing with O_2. Both sequential (A and C) and parallel (B and D) models have been used. Panels A and B show the results in the absence of reducing agent but in the presence of 38 μM O_2. Panels C and D show the spectra in the presence of 3 mM DTT and 138 μM O_2. Error bars are also shown, and typically 3 time constants are needed for a satisfactory fit. The magenta spectrum represents the end spectrum at 500 s. The time constants ($\tau = 1/k$) under given experimental conditions are independent of the applied model (figures A–B and C–D share the same time constants), although the spectra resulting from either model are different. The first spectrum in panels A and C appears with the denoted rate constant k_{AB} in the legend. The black arrows in panels A and B denote the apparent blue shift in the oxidised species to form, we conclude, flavin hydroperoxide (occurring from the red spectrum to the cyan one in panel A, and, conversely, visible in the difference features in the red spectrum in panel B representing the same process).

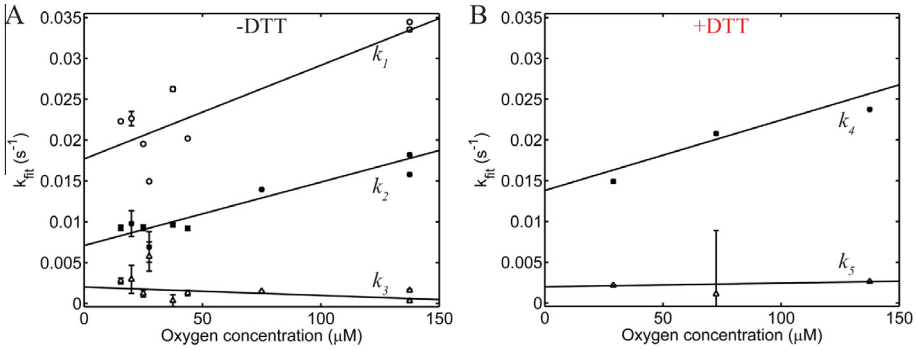

Fig. 4. Rate constant k_{obs} as function of oxygen concentration for the first three rate constants (panel A), yielded by global analysis of the Tris buffer data (without reductant). The two fastest components (open circles and closed squares, corresponding to $k_1 = k_{AD}$ and $k_2 = k_{BD}$, respectively, in Fig. 3B) show a weak oxygen concentration dependence, while the slowest does not (open triangles, corresponding to $k_3 = k_{CD}$ in Fig. 3B), demonstrated by a weighted linear fit applied to each group. The slopes of the fits are $k_1 = 115\ M^{-1}\ s^{-1}$ ($R^2 = 0.77$), $k_2 = 78\ M^{-1}\ s^{-1}$ ($R^2 = 0.87$) and $k_3 = -10\ M^{-1}\ s^{-1}$ ($R^2 = 0.05$). Similarly, panel B shows the rate constants for those obtained in phosphate buffer (with reductant), depicting only the rate constants for the transitions shown in Fig. 5 (the second and third time constants). The slopes of a weighted linear fit are $k_4 = k_{BD}$ (+DTT) = $86\ M^{-1}\ s^{-1}$ ($R^2 = 0.85$) and $k_5 = k_{CD}$ (+DTT) = $5\ M^{-1}\ s^{-1}$ ($R^2 = -0.19$, indicating the inappropriateness of a linear model) for the closed squares and open triangles, respectively. The numbering of the rate constants corresponds to those used in Fig. 5, and both panels depicted here share the same ordinate for easier comparison.

concentration with rate constants of $k_1 = k_{AD} = 115\ M^{-1}\ s^{-1}$ and $k_2 = k_{BD} = 78\ M^{-1}\ s^{-1}$, respectively. The third process $k_3 = k_{CD}$ = is essentially oxygen concentration independent.

In the presence of reductant (see Fig. 3C and D) the fully reduced form reacts with oxygen to yield oxidised cry. The sequential model (Fig. 3C) shows the disappearance of the radical with k_{BC} (+DTT; green spectrum) followed by the appearance (+DTT; with k_{BC}) of a spectrum (red) that shows both radical (maximum absorbance at about 560 nm) and oxidised flavin (maxima at 450 nm and 473 nm) appear with the same time course, followed by the final formation of the oxidised spectrum with k_{CD} (+DTT; cyan spectrum). Analysis of this dataset with the parallel model yields essentially the same spectral information, and the absence of compensating features do not allow to express a preference for either model. Interestingly, the green spectrum in Fig. 3D (and, conversely, the red spectrum associated with the same time constant k_{BC} (+DTT) in Fig. 3C) shows that the oxidised and radical species are transiently formed together with k_{BD} (+DTT) and in approximately equal amounts (the extinction coefficient ratio between oxidised/radical species is about 3 [20,21,24]). It is also worth noting that the spectrum of the radical is identical in spectral distribution in both experiments (with or without reductant, see the green spectrum in Fig. 3B and red spectrum in 3D, respectively), but it is about 3-fold faster in the absence of reductant than in its presence. This difference in rate is remarkable given the fact that the oxygen concentration was lower in the absence of reductant (at 38 μM O_2) than in the presence of reductant (at 138 μM O_2). In addition, the red spectrum in Fig. 3D exhibits features at 367 nm, 426 nm, and 450 nm (with the latter having a wing at 476 nm), and shows remarkable similarities to the sum of the spectra associated with the 42, 107 and long-lived spectra in Fig. 3B (these spectra and its sum is reproduced in Fig. S2 for comparison), meaning that the transiently formed radical in the presence of reductant follows the same pathways as the radical in the absence of reductant.

3. Discussion

Although the reactions between partially and fully reduced cry with oxygen are complex and full mechanistic descriptions are presently not available, the reaction mechanism given in Fig. 5 can account for the essential features of the data we present and will form the basis of the following discussion. This scheme depicts a more complete picture than that given in a previous report [1],

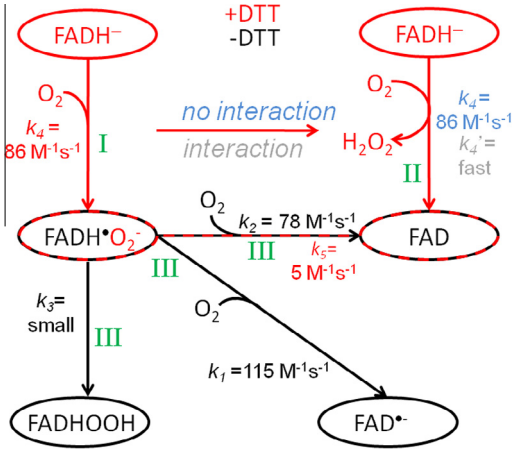

Fig. 5. Proposed reaction schemes for the reaction of oxygen with illuminated cryptochrome in the absence (−DTT; black lines) and presence of reductant (+DTT; red lines). Without reductant, a parallel scheme applies in which the radical disappears with three rate constants (k) to form three different species. Only the radical to flavin hydroperoxide transition (k_3) is oxygen concentration independent. With reductant two parallel non-interacting (k_4) or interacting (k_4') fully reduced populations (implying heterogeneity, or an interacting dimer of which each subunit has a reactivity that depends on the redox state of the partnering subunit) react with oxygen to form the radical in one monomer (reaction I), after which the flavins in a second monomer loose 2 electrons in total to form oxidised flavin (reaction II). In our experiments we find that oxidised and radical flavin appear simultaneously in a 1:1 ratio. The final step (reaction III) is the oxidation of the remaining radical to form the flavin hydroperoxide (k_3), anion flavin radical (k_1) and oxidised flavin (k_2). The shown transitions do not necessarily represent the correct stoichiometry, but highlight the known reactants and products.

as we also present the oxidation pathways in absence of reductant. In order to achieve satisfactory simulations of the data, the scheme includes two pathways from the fully reduced flavin, which could arise from sample heterogeneity or potentially from inter-subunit interaction within the cry dimer. Central to all these simulations is the requirement for radical and oxidised species to form simultaneously from the reaction of photoreduced cry with oxygen in the presence of reductant.

From the results section we conclude that any successful mechanistic model to describe our data should incorporate the following features:

(1) Oxidation of fully reduced cry by oxygen in the presence of reductant yields simultaneously approximately equal concentrations of radical and oxidised flavin, and there is no other process with a distinct time course that transforms fully reduced to oxidised.
(2) Oxidised cry is formed from the radical in the presence or absence of reductant.
(3) Fully reduced flavin transformed to oxidised flavin with two distinct time constants, both oxygen concentration dependent.
(4) The end product of the reaction of fully reduced cry with oxygen in presence of reductant is essentially identical to the starting population of the reactions in the absence of reductant (see Fig. S2).

There are many possible mechanistic schemes that can be written with three redox states (oxidised, radical and fully reduced) and these are presented in the Supplementary information (see Fig. S3) together with concentration profiles (see Fig. S4) derived from simulations. Examination of these time courses show that only a minority exhibit simultaneous production of radical and oxidised species (models 3, 4, 8–12). Furthermore, of these models 3 and 4 can be eliminated because they do not provide for the radical to oxidised transition, and model 12 can be discarded because the spectra show that this transition only occurs once. The remaining models 8–11 have in common that the pool of fully reduced flavin is divided to form the radical and oxidised species. This may be achieved by a single homogenous pool (models 8, 9 and 11) or a heterogeneous pool (model 10) comprising two essentially equal (in 1:1 stoichiometry, see the results section) populations reacting with two identical rate constants to form the radical or oxidised forms.

The coincidence of two identical rate constants ($k_4 = 86\ M^{-1}\ s^{-1}$) may appear unlikely as does the inherent feature in models 8, 9 and 11 that a single pool of reduced flavin reacts with oxygen in two quite distinct ways, because the reduced to oxidised transition involves a proton transfer step while the reduced to radical transition does not. The presence of free flavin next to cry (both fully photoreduced) can be excluded because free flavin typically reacts threefold faster with oxygen [17]. Even in model 10, which can account for the experimental findings and is more fully described in Fig. 5, the occurrence of two identical rate constants to produce radical and oxidised flavin is a feature difficult to explain (depicted in blue in Fig. 5). Perhaps this reflects a somewhat more complex underlying mechanistic feature. For example as it is known that cry is a dimer one might propose that the reduced flavin in each monomeric form is initially identical, but on the reaction of one with oxygen (leading to the radical species) this influences the reactivity of the second such that it reacts extremely rapidly with oxygen to yield directly the fully oxidised species. In this way a radical and oxidised flavin may be produced in equal concentrations and at a rate limited by the initial reaction with oxygen to form the radical species. This suggestion is incorporated in Fig. 5 (depicted in grey). Interaction between subunits of flavoproteins dimers is not unique to cryptochrome. For example, the flavin containing protein nitric oxide synthase (NOS) forms homodimers [37] (similar to (*At*)Cry [38]) that transfer electrons to each other.

In the absence of reductant the reaction of cry with oxygen can also be described by Fig. 5. The starting population is the radical that is an intermediate in the reaction of fully reduced cry with oxygen, except that in the latter case the radical is coordinated with a superoxide molecule, slowing the reaction of the radical to form oxidised flavin (compare rates of formation of the oxidised form in absence and presence of reductant). From the radical a transition to the fully oxidised species (with a rate constant of $k_2 = k_{BD} = 78\ M^{-1}\ s^{-1}$, see Fig. 4A) is observed, and a species that absorbs at 415 nm which we assign to the flavin anion radical (with a rate constant of formation of $k_1 = k_{AD} = 115\ M^{-1}\ s^{-1}$, see Fig. 4A) that typically absorbs at $\lambda_{max} = 380$ nm and 400 nm [24]. This assignment is presently tentative. These rate constants are comparable in magnitude to other flavoproteins such as flavocytochrome ($50\ M^{-1}\ s^{-1}$ [39]), but a factor 2–3 faster than previously reported [1] which probably (predominantly) arises from a non-included dilution factor of 2 in that study (air-saturated buffer contains about 250 μM O_2, just as the highest reported O_2 concentration in said work which also contains oxygen-free buffer). In addition, the blue shift in the oxidised spectrum by 15 nm of a subpopulation of the molecules suggest that the flavinhydroperoxide (see Fig. 3A and B) is formed in a slow process. However, the current data does not allow unequivocal assignment of these species, and ^{13}C NMR labelling studies of C(4a) [40] are needed to confirm the existence of the hydroperoxide form.

The scheme we propose for cry in the presence of oxygen and reductant exhibits several differences compared to earlier studies [1], which may partially be explained by different experimental conditions. For example a 5 times higher salt concentration (0.5 M) was previously used, which may possibly have affected the protein's subunit interaction due to its higher ionic strength [41], although this has not been investigated in detail for crys. Although at the beginning of our experiment the predominant species is the fully reduced form (which remains constant in absence of O_2), a relatively small radical population is also present at time zero, evident by the initial decrease in absorbance assigned to the radical after which the absorbance increases and ultimately declines again (see Fig. 2). These spectral changes have not previously been reported, probably because of the limited available time resolution of the previous studies (apparently in the order of tens of seconds). We argue that with our starting conditions (i.e. concentrations protein/reductant and illumination conditions) a small fraction of the sample does not reach the fully reduced state, and follows the 'reductant-less' pathway. However, the major feature observed, and not noted in earlier studies, is the *simultaneous* formation of high population of radical (reaction I) and oxidised species (reaction II). This finding cannot be accommodated by the simpler scheme proposed earlier in which reduced flavin converts sequentially to the radical and to the oxidised species.

3.1. Cry as magnetosensor

The chemistry of the [O_2] dependent transition from $FADH^{\cdot} \rightarrow FAD$ (in the absence of reductant) poses questions that are relevant for cry and its reported magnetosensitivity which may involve a superoxide-$FADH^{\cdot}$ radical pair. The reaction of photoreduced cry and oxygen in the absence of reductant generates FADHOOH (Fig. 3A and B), formed by the interaction of $FADH^{\cdot}$ with superoxide, itself produced by donation of an electron to oxygen possibly from a Trp residue, from the dimer partner, or both. In contrast, it is the flavin chromophore that donates the electron to molecular oxygen for photoreduced cry in the presence of reductant. The magnetosensitive radical pair that is formed depends therefore on the redox state of the flavin chromophore.

The work presented here provides evidence for the involvement of superoxide, being produced from the fully reduced state, or leading to the formation of FADHOOH from the semiquinone state (see Fig. 5). Radical pairs such as the $FADH^{\cdot}O_2^{-}$ complex are a candidate for the magnetosensitive radical pair, although recent investigations suggest that reaction of triplet dioxygen with fully reduced flavin or superoxide with a flavin radical (both forming a complex between photoreduced flavin and oxygen) may not result in an observable magnetosensitive response [42]. The $FADH^{\cdot}O_2^{-}$ complex can however still not be fully excluded as suitable candidate.

Simulations have also tentatively suggested the ascorbyl radical, of which its origin remains unknown, as alternative radical pair partner [43]. Despite the fact that this work has implications for cry's function as magnetosensor, its physiological relevance may be limited, as the second antenna chromophore (which, as in nitric oxide synthase [37], possibly plays an active role in cry's radical chemistry) may be an essential factor in directing the electron flow in cry.

4. Conclusions

It is shown that *At*Cry can be photoreduced under anaerobic conditions, and can be oxidised by molecular oxygen through a number of oxygen concentration dependent and independent pathways. Global analysis reveals that the reaction of the fully reduced form with molecular oxygen displays the simultaneous formation of the radical and oxidised species, which is not consistent with a simple sequential model and requires a more complex mechanism. This suggests that there are different cryptochrome molecules with different reactivities, or that the reactivity of each subunit of the cryptochrome dimer depends on the redox state of the partnering subunit. In the absence of reductant photoreduced cry most likely forms a flavin hydroperoxide requiring superoxide. The latter is formed by molecular oxygen that, depending on the redox state of the flavin, receives an electron from the reduced flavin, or from within the protein (likely to be a Trp residue, and/or from the dimer partner).

The presented results offer a more complete picture of the reaction mechanisms of photoreduced cryptochrome with molecular oxygen, and confirms that superoxide is involved in the oxidation pathway which may be relevant for cry's function as possible magnetoreceptor. The validity of this hypothesis can be tested by undertaking magnetic field experiments on cry under controlled oxygen concentrations.

5. Materials and methods

5.1. Sample preparation

Protein was prepared as previously described in [2]. The final used sample absorbance is ~60–100 mOD at 445 nm, which corresponds to a few μM of protein. Samples were kept on ice. Two types of buffers are used: 0.1 M Tris–HCl pH 7.5, 0.1 M NaCl, and 0.1 M phosphate buffer-HCl pH 7.5, 0.1 M NaCl.

To study the interaction of oxygen and cry, and to unravel its underlying redox chemistry, sample conditions are initially kept as simple as possible, i.e. remaining imidazole (from the protein purification process), free flavin (potentially fallen out from the protein), and glycerol are removed by running the protein over a gel filtration column (Sephadex G-25), and we refrain from using oxygen scavengers (see below), but add reductant (taken from a 0.5 M DTT stock solution) if the fully reduced form needs to be produced. The presented phosphate buffer samples with reductant are done with 3 mM DTT.

5.2. Stopped flow apparatus

The kinetics of oxidation of photo-reduced cry were determined by mixing anaerobic illuminated cry (5 min irradiation with a 470 nm Philips Lumileds LED) with oxygen containing buffer in a stopped-flow apparatus (SX20, Applied Photophysics, UK). The anaerobic samples (produced by blowing N_2 over the liquid–air surface for ~30 min, and leaving a slight N_2-overpressure) are yellow, and were loaded in glass syringes (with greased stems to prevent oxygen from entering the solution) and consequently illuminated outside the apparatus until visibly colourless. If the sample turned yellow again (due to remaining oxygen), the procedure was repeated until it remained colourless (i.e. until the oxygen was consumed). Moreover, the colour of the solution was checked inside the apparatus as well in order to monitor oxygen leaks. The time courses were followed by recording the absorption difference spectrum (with respect to time zero, i.e. for the samples with reductant the predominantly fully reduced flavin state is subtracted, for the samples in absence the predominantly radical flavin state) at 1.25 s intervals as a function of time. The used optical pathlength is 10 mm, and the measurement chamber (at about 25 °C) has a volume of 20 μL. The probe light is generated by a Deuterium lamp, and dispersed on a 256 element array, resulting in a wavelength resolution of about 3.3 nm. Buffers of known oxygen concentration were made by mixing degassed buffer (generated by degassing for 10–15 min in a tonometer) with the desired volumes of air-equilibrated buffer, the oxygen concentration of which was determined from the solubility coefficient and corrected for temperature (22 °C) and atmospheric pressure (~1010 hPa) [44]. As it is virtually impossible to go to zero oxygen concentration without using oxygen scavengers (which can potentially interact with cry), the lowest oxygen concentration used is about 16 μM. Shorter illumination times (3 vs 5 min.), or increasing the time resolution (24 ms vs 1.25 s) gave the same results. Three independent sample preparations and measurements gave consistent and repeatable (at least 4 times for each oxygen concentration) results. The difference absorbance spectra (measured up to 8 min.) show no evidence of aggregate formation (which would show a dramatic increase in absorbance at lower wavelengths on a time scale of hours [45]). Control experiments confirmed that the probe light did not photoreduce the sample.

5.3. Data analysis

Global analysis of the spectral changes following mixing cry with oxygen was performed using the Globe Toolbox described in Ref. [46]. For this analysis the spectra were corrected for scatter or any small absorbance drift [44,47] by setting the absorbance at 700 nm (a wavelength where cry does not absorb) at zero. A positive band thus represents the formation of a product or intermediate state, while a negative band corresponds to the disappearing starting state [48,49].

The fitting procedure entailed the application of two models to the data (i.e. a parallel model, involving a sum of exponentials, or a sequential model, where the decay of one exponential determines the growth of the next population). This approach renders it possible to extract time-independent spectra associated with a specific lifetime, and to determine if the appearance or disappearance of two species is temporally correlated. The quality-of-fit is judged based on the sum-of-squares of the residuals value (fit-minus-data; only an additional time constant is added when accompanied by a significant reduction in this value), and on the absence of structure in the residuals in the time and in the spectral domain. Although the spectra resulting from a global analysis by using either model are different, the associated time constant are identical. A restraint on determining the actually occurring model is provided by noting that spectral compensation (i.e. the spectral signature of one species is mirrored by that of another species) indicates an inappropriate model for that transition.

5.4. Kinetic simulations

Modelling of concentration profiles for a selection of connectivity schemes is done using the SimBiology Toolbox in Matlab [50]. Each transition is associated with an exponential function.

Author contributions

L.J.G.W.v.W., J.J.v.T. and M.W.T. planned the experiments, L.J.G.W.v.W., G.S., M.S. and M.T.W. performed the experiments, L.J.G.W.v.W. and M.W.T. analysed the data, L.J.G.W.v.W., J.J.v.T. and M.T.W. wrote the paper.

Acknowledgments

L.J.G.W.v.W. thanks the Federation of Biochemical Sciences (FEBS) for funding via a Long-Term Fellowship. M.T.W. and G.S. thank the Electric and Magnetic Field Biological Research Trust for funding. All authors thank M. Ahmad of the University of Paris VI (France) for supplying the protein samples and the reviewers for their helpful and constructive dialogue.

Appendix A. Supplementary data

Supplementary data associated with this article can be found, in the online version, at http://dx.doi.org/10.1016/j.fob.2015.10.007.

References

[1] Müller, P. and Ahmad, M. (2011) Light activated cryptochrome reacts with molecular oxygen to form a flavin-superoxide radical pair consistent with magnetoreception. J. Biol. Chem. 286, 21033–21040.
[2] Bouly, J., Schleicher, E., Dionisio-Sese, M., Vandenbussche, F., Van Der Straeten, D., Bakrim, N., Meier, S., Batschauer, A., Galland, P., Bittl, R. and Ahmad, M. (2007) Cryptochrome blue light photoreceptors are activated through interconversion of flavin redox states. J. Biol. Chem. 282, 9383–9391.
[3] Banerjee, R. and Batschauer, A. (2005) Plant blue-light receptors. Planta 220, 498–502.
[4] Cashmore, A.R. (2006) Cryptochromes in: Photomorphogenesis in Plants and Bacteria (Schafer, E. and Nagy, F., Eds.), Springer, Dordrecht, The Netherlands.
[5] Lin, C.T. and Todo, T. (2005) The cryptochromes. Genome Biol. 6.
[6] Malhotra, K., Kim, S.T., Batschauer, A., Dawut, L. and Sancar, A. (1995) Putative blue-light photoreceptors from arabidopsis-thaliana and sinapis-alba with a high-degree of sequence homology to DNA photolyase contain the 2 photolyase cofactors but lack DNA-repair Activity. Biochemistry 34, 6892–6899.
[7] Selby, C.P. and Sancar, A. (2006) A cryptochrome/photolyase class of enzymes with single-stranded DNA-specific photolyase activity. Proc. Natl. Acad. Sci. U. S.A. 103, 17696–17700.
[8] Sancar, A. (2003) Structure and function of DNA photolyase and cryptochrome blue-light photoreceptors. Chem. Rev. 103, 2203–2237.
[9] Lin, C.T., Robertson, D.E., Ahmad, M., Raibekas, A.A., Jorns, M.S., Dutton, P.L. and Cashmore, A.R. (1995) Association of flavin adenine-dinucleotide with the arabidopsis blue-light receptor Cry1. Science 269, 968–970.
[10] Giovani, B., Byrdin, M., Ahmad, M. and Brettel, K. (2003) Light-induced electron transfer in a cryptochrome blue-light photoreceptor. Nat. Struct. Biol. 10, 489–490.
[11] Heelis, P.F. and Sancar, A. (1986) Photochemical properties of *Escherichia coli* DNA photolyase – a flash-photolysis study. Biochemistry 25, 8163–8166.
[12] Banerjee, R., Schleicher, E., Meier, S., Viana, R.M., Pokorny, R., Ahmad, M., Bittl, R. and Batschauer, A. (2007) The signaling state of Arabidopsis cryptochrome 2 contains flavin semiquinone. J. Biol. Chem. 282, 14916–14922.
[13] Hoang, N., Schleicher, E., Kacprzak, S., Bouly, J., Picot, M., Wu, W., Berndt, A., Wolf, E., Bittl, R. and Ahmad, M. (2008) Human and Drosophila cryptochromes are light activated by flavin photoreduction in living cells. PLoS Biol., http://dx.doi.org/10.1371/journal.pbio.0060160.
[14] Berndt, A., Kottke, T., Breitkreuz, H., Dvorsky, R., Hennig, S., Alexander, M. and Wolf, E. (2007) A novel photoreaction mechanism for the circadian blue light photoreceptor Drosophila cryptochrome. J. Biol. Chem. 282, 13011–13021.
[15] Immeln, D., Weigel, A., Kottke, T. and Lustres, J. (2012) Primary events in the blue light sensor plant cryptochrome. J. Am. Chem. Soc. 134, 12536–12546.
[16] Thompson, C.L. and Sancar, A. (2002) Photolyase/cryptochrome blue-light photoreceptors use photon energy to repair DNA and reset the circadian clock. Oncogene 21, 9043–9056.
[17] Massey, V. (1994) Activation of molecular-oxygen by flavins and flavoproteins. J. Biol. Chem. 269, 22459–22462.
[18] Palfey, B.A., Ballou, D.P. and Massey, V. (1995) Oxygen activation by flavins and pterins in: Active Oxygen in Biochemistry (Valentine, J.S., Foote, C.S., Greenberg, A. and Liebman, J.F., Eds.), Springer Netherlands.
[19] Mattevi, A. (2006) To be or not to be an oxidase. Trends Biochem. Sci. 31, 276–283.
[20] Dawson, R. (1986) Data for Biochemical Research, third ed, Clarendon Press, Oxford, UK.
[21] Whitby, L.G. (1953) A new method for preparing flavin-adenine dinucleotide. Biochem. J. 54, 437–442.
[22] Hemmerich, P., Veeger, C. and Wood, H. (1965) Progress in the chemistry and molecular biology of flavine and flavocoenzymes. Angew. Chem. Int. Ed. 77, 699–716.
[23] Choong, Y.S. and Massey, V. (1980) Stabilization of lactate oxidase flavin anion radical by complex formation. J. Biol. Chem. 255, 8672–8677.
[24] Müller, F., Brüstlein, M., Hemmerich, P., Massey, V. and Walker, W.H. (1972) Light-absorption studies on neutral flavin radicals. Eur. J. Biochem. 25, 573–580.
[25] Malhotra, K., Kim, S.T. and Sancar, A. (1994) Characterization of a medium wavelength type DNA photolyase – purification and properties of photolyase from bacillus-firmus. Biochemistry 33, 8712–8718.
[26] Sancar, A. (1994) Structure and function of DNA photolyase. Biochemistry 33, 2–9.
[27] Maffei, M.E. (2014) Magnetic field effects on plant growth, development, and evolution. Front. Plant Sci. 5, 445.
[28] Ritz, T., Adem, S. and Schulten, K. (2000) A model for photoreceptor-based magnetoreception in birds. Biophys. J. 78, 707–718.
[29] Nießner, C., Denzau, S., Stapput, K., Ahmad, M., Peichl, L., Wiltschko, W. and Wiltschko, R. (2013) Magnetoreception: activated cryptochrome 1a concurs with magnetic orientation in birds. J. R. Soc. Interface 10, 20130638.
[30] Solov'yov, I.A. and Schulten, K. (2009) Magnetoreception through cryptochrome may involve superoxide. Biophys. J. 96, 4804–4813.
[31] Walsh, C. (1978) Chemical approaches to the study of enzymes catalyzing redox transformations. Ann. Rev. Biochem. 47, 881–931.
[32] Bargon, J., Fischer, H. and Johnsen, U. (1967) Kernresonanz-emissionslinien während rasher Radikalreaktionen. I. Aufnahmeverfahren und Beispiele. Z. Naturforsch. A 22, 1551–1555.
[33] Berg, J.M., Stryer, L. and Tymoczko, J.L. (2002) Biochemistry, Ch. 8, fifth ed, W. H. Freeman, New York.
[34] Liochev, S.I. and Fridovich, I. (2004) Carbon dioxide mediates Mn(II)-catalyzed decomposition of hydrogen peroxide and peroxidation reactions. Proc. Natl. Acad. Sci. U.S.A. 101, 12485–12490.
[35] Chaiyen, P., Sucharitakul, J., Svasti, J., Entsch, B., Massey, V. and Ballou, D.P. (2004) Use of 8-substituted-FAD analogues to investigate the hydroxylation mechanism of the flavoprotein 2-methyl-3-hydroxypyridine-5-carboxylic acid oxygenase. Biochemistry 43, 3933–3943.
[36] Palfey, B.A., Murthy, Y.V. and Massey, V. (2003) Altered balance of half-reactions in p-hydroxybenzoate hydroxylase caused by substituting the 2′-carbon of FAD with fluorine. J. Biol. Chem. 278, 22210–22216.
[37] Alderton, W.K., Cooper, C.E. and Knowles, R.G. (2001) Nitric oxide synthases. Biochem. J. 357, 593–615.
[38] Sang, Y., Li, Q.H., Rubio, V., Zhang, Y.C., Mao, J., Deng, X.W. and Yang, H.Q. (2005) N-terminal domain-mediated homodimerization is required for photoreceptor activity of Arabidopsis cryptochrome 1. Plant Cell 17, 1569–1584.
[39] Boubacar, A.K.O., Pethe, S., Mahy, J.P. and Lederer, F. (2007) Flavocytochrome b (2). Biochemistry 46, 13080–13088.
[40] Vervoort, J., Muller, F., Lee, J., Van den Berg, W.A.M. and Moonen, C.T.W.M. (1986) Identifications of the true carbon-13 nuclear magnetic resonance spectrum of the stable intermediate II in bacterial luciferase. Biochemistry 25, 8062–8067.
[41] Wu, D., Hu, Q., Yan, Z., Chen, W., Yan, C., Huang, X., Zhang, J., Yang, P., Deng, H., Wang, J., Deng, X. and Shi, Y. (2012) Structural basis of ultraviolet-B perception by UVR8. Nature 484, 214–219.
[42] Hogben, H.J., Efimova, O., Wagner-Rundell, N., Timmel, C.R. and Hore, P.J. (2009) Possible involvement of superoxide and dioxygen with cryptochrome in avian magnetoreception: origin of Zeeman resonances observed by in vivo EPR spectroscopy. Chem. Phys. Lett. 480, 118–122.
[43] Lee, A.A., Lau, J.C.S., Hogben, H.J., Biskup, T., Kattnig, D.R. and Hore, P.J. (2014) Alternative radical pairs for cryptochrome-based magnetoreception. J. R. Soc. Interface 11, 20131063.
[44] Wagner, W. and Pruss, A. (1993) International equations for the saturation properties of ordinary water substance – revised according to the international temperature scale of 1990 (Vol 16, Pg 893, 1987). J. Phys. Chem. Ref. Data 22, 783–787.
[45] Penzkofer, A., Shirdel, J., Zirak, P., Breitkreuz, H. and Wolf, E. (2007) Protein aggregation studied by forward light scattering and light transmission analysis. Chem. Phys. 342, 55–63.
[46] van Wilderen, L.J.G.W., Lincoln, C.N. and van Thor, J.J. (2011) Modelling multi-pulse population dynamics from ultrafast spectroscopy. PLoS ONE 6, e17373.
[47] Holler, F.J., Enke, C.G. and Crouch, S.R. (1980) Critical-study of temperature effects in stopped-flow mixing systems. Anal. Chim. Acta 117, 99–113.
[48] Ruckebusch, C., Sliwa, M., Pernot, P., de Juan, A. and Tauler, R. (2012) Comprehensive data analysis of femtosecond transient absorption spectra: a review. J. Photochem. Photobiol., C 13, 1–27.
[49] van Stokkum, I.H.M., Larsen, D.S. and van Grondelle, R. (2004) Global and target analysis of time-resolved spectra. Biochim. Biophys. Acta Bioenergy 1657, 82–104.
[50] MATLAB, The MathWorks Inc, Natick, Massachusetts, United States.